Rauch, Cyril and Cherkaoui-Rbati, Mohammed (2014) Physics of nail conditions: why do ingrown nails always happen in the big toes? Physical Biology, 11 (6). 066004/1-066004/10. ISSN 1478-3975

Physics of nail conditions: why do ingrown nails always happen in the big toes?

2014 Phys. Biol. 11 066004

(http://iopscience.iop.org/1478-3975/11/6/066004)

OPEN ACCESS
IOP Publishing
Physical Biology
Phys. Biol. 11 (2014) 066004 (10pp)
doi:10.1088/1478-3975/11/6/066004

Physics of nail conditions: why do ingrown nails always happen in the big toes?

Cyril Rauch and Mohammed Cherkaoui-Rbati

School of Veterinary Medicine and Science, University of Nottingham, College Road, Sutton Bonington, LE12 5RD, UK

E-mail: Cyril.rauch@nottingham.ac.uk

Received 10 June 2014
Accepted for publication 12 August 2014
Published 16 October 2014

Abstract

Although surgical treatment of nail conditions can be traced back centuries to the writings of Paul Aegineta (625–690 AC), little is known about the physical laws governing nail growth. Such a poor understanding together with the increasing number of nail salons in the high street should raise legitimate concerns regarding the different procedures applied to nails. An understanding of the physics of nail growth is therefore essential to engage with human medicine and to understand the aetiology of nail conditions. In this context, a theory of nail plate adhesion, including a physical description of nail growth can be used to determine the transverse and longitudinal curvatures of the nail plate that are so important in the physical diagnosis of some nail conditions. As a result physics sheds light on: (a) why/how nails/hooves adhere strongly, yet grow smoothly; (b) why hoof/claw/nail growth rates are similar across species; (c) potential nail damage incurred by poor trimming; (d) the connection between three previously unrelated nail conditions, i.e. spoon-shaped, pincer and ingrown nails and; last but not least, (e) why ingrown nails occur preferentially in the big toes.

Keywords: hard and growing tissues, biomechanics, dermatology, adhesion

Introduction

The human nail is a keratinized structure and window to the nail bed, held in place by lateral nail folds (the cutaneous folded structures providing the lateral borders of the nail). It is made of dead cells that multiply from the proximal matrix. As a result, the nail originates from this proximal matrix, grows longitudinally, and ends at a free edge distally. Nail adhesion to the nail bed involves a number of well characterised microscopic adhesive units. These units are apposed in a pattern along longitudinal epidermal ridges (or lamellae) stretching to the lunula, the half moon, pale convex portion of the matrix seen through the nail (figure 1(A)). On the underside of the nail plate there is a complementary set of ridges as if the nail plates were held to the nail beds via a set of longitudinal rails. A similar anatomical structure exists across all species. However, depending on the animal considered, the epidermal ridges can be more complex than in man as they can display primary *and* secondary structures that are thought to increase adhesiveness. For example, slow-moving animals like humans and cattle have only primary lamellae (Thoefner *et al* 2005) whereas fast-moving animal like horses (Pollitt 1994) or heavy animals like elephants (Benz *et al* 2009) have primary and secondary lamellae (figures 1(B), (C), (D) and (E) show the horse foot as an example).

Even though there now exists an in depth and complex cross-species description of macroscopic/microscopic anatomical and cellular/sub-cellular structures, how nail and hoof growth inform their shape remains unclear. This apparently simple question is in fact central to medicine as the first diagnosis of a nail/hoof condition by medics or vets is necessarily a physical and visual appraisal of the shape or form of the nail/hoof. In this context it is worth noting that although nail cutting and hoof trimming have traditionally been advocated to alleviate pain and reshape the nail/hoof with time, there is little theory on which to ground these

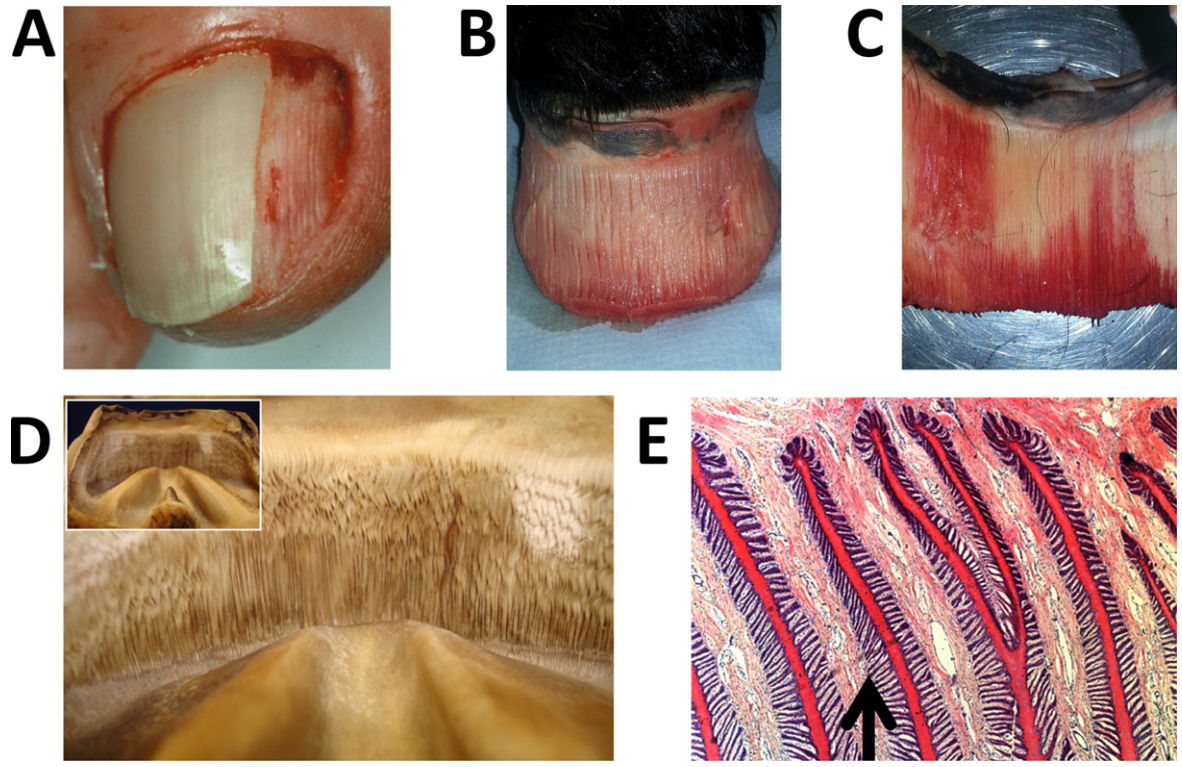

Figure 1. Anatomy of nail and hoof adhesion. **(A)** Avulsion of the human nail showing the nail bed and in particular the epidermal ridges interacting with the nail plate (figure reproduced from de Berker, Andre and Baran 2007). The anatomy of the epidermal structures is similar across species. **(B)** Avulsion of the equine hoof capsule showing the bed and in particular the epidermal ridges interacting with the hoof capsule. (The material was obtained from an ethically managed abattoir). **(C)** Internal view of epidermal ridges separated from foot (B). **(D)** Internal view of dried epidermal ridges. **(E)** A microscopic section shows that in addition to the first lamellae (pink colour) there is a second one (dark blue/dark purple colour pointed by the black arrow) that is connected to the hoof capsule (red colour). The hoof-lamellar interface increases the surface area for adhesion.

practices (Eliashar 2012). Furthermore, for each shape-related condition, it is unclear whether another cutting/trimming method exists that could be optimized. As a result, if a connection exists between the zoology of nail shapes and the zoology of nail conditions, it is paramount to describe how these changes have been made possible and what 'physical' parameters are involved. These parameters should help to define the aetiology of nail/hoof conditions and give valuable clues as to how they should be treated.

The present work considers the nail as an adhering solid plate and will start by a brief hand-waiving introduction of physical concepts used. The adhesion and growth stresses present in nail will be modelled and incorporated into the general balance of stresses to obtain unique solutions. The optimization of the total energy of the nail including bending and potential energies will be performed using the Euler–Lagrange method to determine the nail shape equation. The nail shape equation will be tested against specific nail conditions where changes in the shape of the affected nail occur. We conclude that our model may provide a continuous relationship between three well known, but previously thought to be unrelated, nail conditions namely ingrown, pincer and spoon-shaped nails. Finally we shall also discuss the potential importance of nail cutting in the aggravation of nail conditions.

Model

Below we explain the different concepts that will be used. As a nail is a growing solid that adheres to a substrate, the adhesion of the nail plate on its bed is necessarily involved in the way it grows. Adhesion between cells and the extracellular matrix is formed via specialized junctions involving different sets of macro-molecules including more complex ones such as focal adhesion or hemi-desmosomes (Worth and Parsons 2008). Cellular adhesion has been extensively modelled in different contexts. As a function of the biology considered, the frameworks can differ, but intermolecular bonds forming adhesions are usually treated as Hookean springs that can either remain fixed vertically (Dembo *et al* 1988, Dong and Lei 2000) and/or tilt from their vertical position under stress (Reboux *et al* 2008). As a nail adheres strongly, but needs to grow smoothly (i.e. without stick-slip), one possibility is that this adhesion imposes a ratchet-like mechanism on the nail so that the 'growth' is essentially confounded with diffusion. This is possible if the length of nail growth per unit of time has a magnitude that is similar to the thermal tilting of an adhesive unit. In these conditions the adhesive units should not 'feel' the nail to which they are bound, and a nail should grow smoothly and adhere strongly. This ratchet-like model

indicates a universal form of growth for hooves and nails in non-pathological conditions but it needs to be amended when the growth rate of the keratinized plate is too fast. In this case, the adhesive forces opposing the nail plate movement and the mechanics of the plate need to be considered together. To understand clearly how mechanical stresses arise, it is essential to understand the mechanical impact of the nail edge as a boundary condition.

To explain this let us isolate a thin longitudinal slab of the nail plate, from the proximal matrix to the free end. As the pink colour underneath the slab is proportional to the number of adhesive units involved in the adhesion of the slab, the longer the slab the higher the adhesion. As a result, with a constant growth force emanating from the proximal matrix, the longer the slab the harder it will be to make it move forward or grow. Thus, given the parabola-like shape where the adhesion of the nail terminates, the right and left extremities of the nail of a thumb should grow faster than the longitudinal slab positioned exactly in its center because the latter would be longer than any other slab. Naturally, this is never observed as the nail has solid properties. Nevertheless it describes the set of residual longitudinal shear stresses involved when the nail grows that result directly from the boundary conditions. As a longitudinal shear stress promotes a tendency toward rotation (i.e. to generate angular momentums) but because nails do not rotate locally, another stress, transverse this time, must balance the virtual rotation primed by the shear stress. This transverse stress resulting from the profile of the nail edge, is expected to have an impact on the transverse curvature of the nails, which is important in the diagnosis of nail conditions.

Thermal growth rate

To provide a model, let us first focus on a single adhesive unit that stands vertically without solicitation of any sort. Single molecular adhesion can only last a time $\sim 1/k_-$ where, k_-, is the unbinding kinetic (figure 2(A)). If, when the adhesive unit has just bonded, a movement involving a constant velocity, V, is now imposed on the unit and that the unit is fully compliant mechanically, the unit will tilt up to a certain angle, θ, before unbinding. This angle is expected to be, $\theta \sim V/z_0 k_-$ (figure 2(B)). The thermal agitation of any free, i.e. unbound, unit can also define an angle proportional to the absolute temperature, $k_{el}\left\langle \theta^2 \right\rangle \sim k_B T$, where k_{el} is the tilt modulus of the unit, k_B the Boltzmann's constant and T, the absolute temperature (figure 2(C)). Equating the two relations allows one to define a thermal velocity:

$$V_{th} \sim z_0 k_- \sqrt{k_B T / k_{el}} \tag{1}$$

This velocity defines a limit below which adhesion/binding is controlled by the thermal energy. This means that the movement of a nail plate onto adhesive units is possible without further damage of units other than those determined thermally if the velocity is close to, or below, V_{th}. Using $k_{el} \sim 10 - 10^3\, k_B T$ (Reboux, Richardson and Jensen 2008), $k_- \sim 10 s^{-1}$ (Ra *et al* 1999) and $z_0 \sim 10$ nm (Arnold *et al* 2004, Cavalcanti-Adam *et al* 2006, Cavalcanti-Adam *et al* 2007) one finds $V_{th} \sim 0.1-1$ mm/*day* at room temperature. The growth rate of nail/hoof/claw measured in a range of species (table 1) falls within the range of thermal velocities that can be predicted by this model. In addition, the very close similarity between growth rates *in-vivo* suggests that physics drives the process of growth. Indeed these *in-vivo* values are not dependent on allometric properties and, as a result, do not seem to involve the species–species metabolic rates, at least under normal conditions.

Binding probability of adhesive units

Above the thermal velocity the probability that a unit remains attached becomes a function of the stress imposed on the unit. In this context, consider as above a single adhesive unit that stands vertically without solicitation of any sort. Once bound with a chemical energy, ΔE_0, the thermal escape rate from the bound state is $k_- \sim e^{-\Delta E_0/k_B T} f_0$ where, f_0, is a fundamental frequency. Upon movement of the nail the unit tilts and the energy landscape changes. In this context the unit has two possibilities, to remain bound or to break and as a result the transition rate between the 'bound' and 'unbound' states is: $f_- \sim e^{-\left(\Delta E_0 - k_{el}\theta^2/2\right)/k_B T} f_0$. Considering independent and identical adhesion units, a kinetic model can be used to describe the probability, P, that a unit is attached over time:

$$dP/dt = -f_- \times P + k_+ \times (1 - P) \tag{2}$$

where k_+ is the binding rate. The last term on the right-hand-side of equation (2) represents the probability that an adhesive unit rebinds after unbinding. In this case, the relaxation time relating to the adhesive unit going from a stretched state to its resting position before rebinding is neglected. The later relation also assumes that there is no competition between binding sites and that a reservoir of ligands exists so that the binding can be considered spatially continuous. Considering a steady state regime of growth, i.e. $dP/dt = 0$, it follows:

$$P\left(\overline{V}\right) = \left[1 + \alpha \exp\left(\overline{V}^2/2\right)\right]^{-1} \tag{3}$$

where $\overline{V} = V/V_{th}$ and $\alpha = k_-/k_+$ (figure 2(D)). Equation (3) shows the sensitivity of $P\left(\overline{V}\right)$ with regard to the growth rate of nails.

Adhesion force developed by adhesive units

Focusing on a single adhesion unit, the force that opposes the growth can be determined trivially as: $k_{el} V_{th}/z_0^2 k_- \times \overline{V} P\left(\overline{V}\right)$. Consider a small element of nail surface area, the adhesion per unit of surface of nail is thus: $f_{adh}(V) = k_{el} V_{th}/z_0^2 k_- \times \rho \overline{V} P\left(\overline{V}\right)$ (figure 2(E)), where ρ is the number of adhesive units per surface area of nail that will

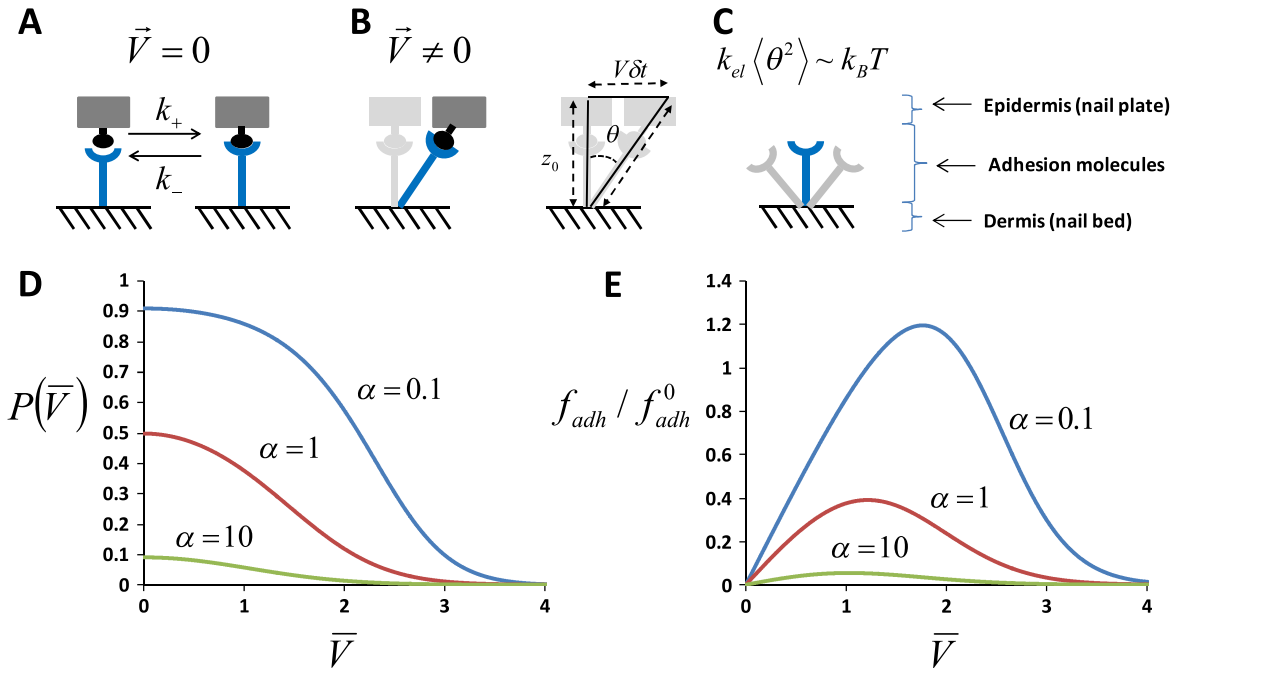

Figure 2. Adhesion and growth force. **(A)** Adhesive units bind and unbind to their ligand over time. In a steady state regime, with no velocity involved, the bound and unbound states can be described by a basic 2 states model. **(B)** When the nail grows, the binding of the adhesive units last until a certain value of the titling angle is reached, that is determined thermally or mechanically depending on the regime considered. **(C)** When the adhesive unit is not bound, the tilt fluctuates around the vertical position and the use of thermodynamics allows one to determine the deviation from the average value. **(D)** Representation of the probability that a bond is not consumed as a function of the growth rate and α. **(E)** Representation of the force generated by a bound adhesive unit as a function of the growth rate and α.

Table 1. Hoof/nail growth rates for different animal species.

Animal	Growth rate (mm day^{-1})	References
Horse	0.2–0.3	(Butler and Hintz 1977)
Sheep	0.1–0.2	(Shelton *et al* 2012)
Deer	0.1–0.2	(Miller *et al* 1986)
Cow	0.1–0.3	(Harrison *et al* 2007, Telezhenko *et al* 2009)
Elephant	0.1–0.3	(Benz, Zenker, Hildebrandt, Weissengruber, Eulenberger and Geyer 2009)
Pig	0.3–0.4	(Johnston and Penny 1989)
Rat	0.1–0.2	(Godwin 1959)
Human	0.1–0.2	(de Berker, Andre and Baran 2007)

be considered constant and $f^0_{adh}=k_{el}V_{th}/z_0^2k_-\sim 10\,pN$. Note that as the nail plate is a projection of the nail bed and that avulsion of the nail plate reveals a pattern of longitudinal epidermal ridges involved in adhesion (figure 1), the 'true' total surface area available for adhesion is larger than the visible surface of the nail plate and as a result a factor, λ, needs to be introduced to determine the true number of adhesive units per unit of surface area to draw comparisons between species. In these conditions:

$$f_{adh}(V)=f^0_{adh}\lambda\rho\bar{V}P(\bar{V}) \qquad (3a)$$

Balance of in-plane stresses

The adhesive stress being defined, plate mechanics theory can now be used to start investigating the interaction between the shape and adhesion of nails.

The nail is held in place by an adhesion stress and a boundary stress generated by the skin folds. However, as the change of nail shape is expected to be slow, the deformation of the nail bed and related impact on the adhesion stress normal to the nail bed is unlikely to intervene actively in the process, suggesting that we can consider the adhesion stress constant at least for moderate deformations. In addition, as the full characterisation of the external stresses applied by the skin folds on the boundary of nail are, for the moment, unknown to us, we shall only focus on a nail plate that is free from external stresses induced by skin folds.

Consider the in-plane description and a nail plate orientated in such a way that the y-axis corresponds to the direction of growth from the proximal to the distal parts and an x-axis orthogonal to the y-axis along the proximal matrix (figure 3(A)). Let us assume that the nail has a width, l, a length, $h'(x)$, with a constant thickness, e. The initial 3D stress tensor, $[\sigma_{i,j}]$, can be reduced to a two dimensional stress tensor: $\left[f_{i,j}(x,y)\right]=\begin{bmatrix} f_{x,x}(x,y) & f_{x,y}(x,y) \\ f_{y,x}(x,y) & f_{y,y}(x,y)\end{bmatrix}$ with: $f_{i,j}=\int_{-e/2}^{e/2}\sigma_{i,j}dz$ where $f_{i,j}$ is defined as a force per unit of length along the 'j'-axis with direction along the 'i'-axis (figure 3(B)). Note that the terms on the diagonal define

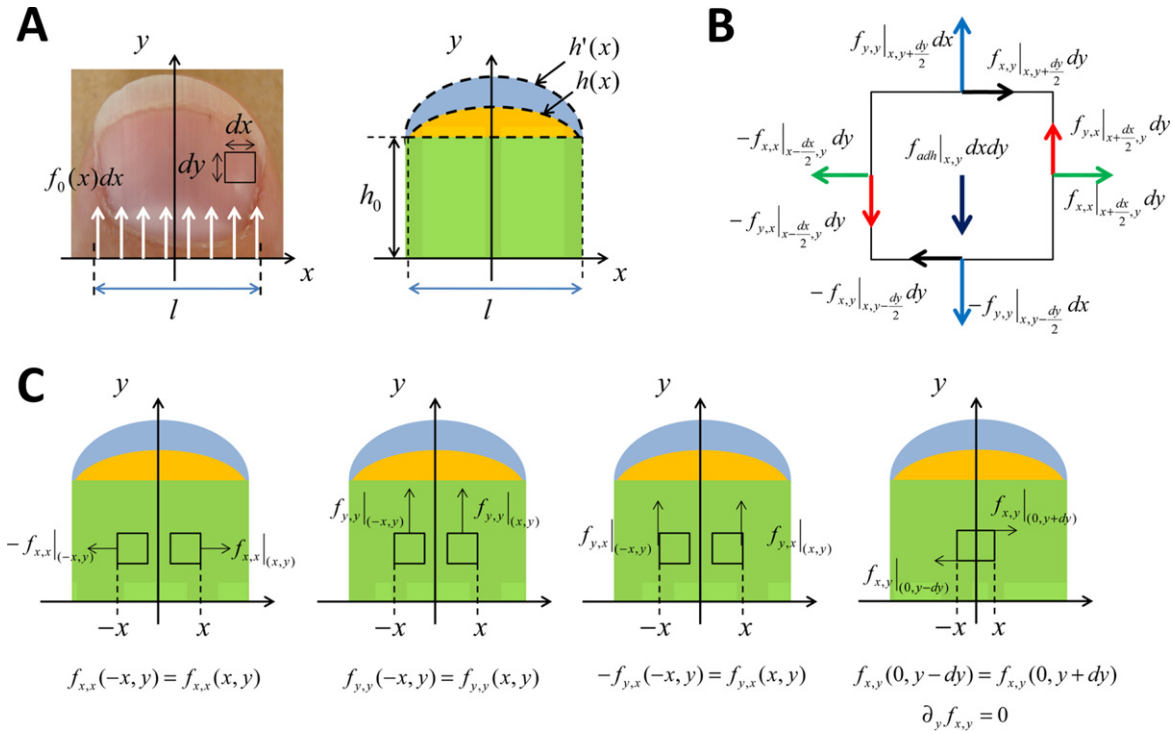

Figure 3. Nail characteristics. **(A)** The nail is described by a system of axes allowing a simple analytic representation. $h(x)$ is the adhesion profile i.e. the upper boundary between the white and pink parts (i.e. delimiting the yellow region from the blue one), and $h'(x)$ the most distal part of the nail (i.e. delimiting the blue region from the outside). These profiles are symmetrical and will be expressed by polynomials involving even functions only. For a clearer representation, h_0 corresponds to the limit of the green area from the proximal matrix. **(B)** Representation of the set of stresses applied to the element of surface dxdy. **(C)** Results concerning the symmetry analysis. The stress tensor can be used on every side of the small square dxdy to determine the conditions of symmetry with regard to the set of forces applied to the nail. Given the balance of angular momentums we will further assume that $\partial_y f_{x,y}$ is also equal to zero everywhere on the x-axis. This is equivalent of considering that the shear stress along a longitudinal slab is constant (does not change much at the lowest order) along the y-axis.

the classical surface tension whereas the non diagonal terms define the shear stresses. Finally, the balance of stresses on an element of surface $dxdy$ of the nail can be written as:

$$\partial_x f_{x,x}(x,y) + \partial_y f_{x,y}(x,y) = 0 \tag{4}$$

$$\partial_y f_{y,y}(x,y) + \partial_x f_{y,x}(x,y) - f_{adh}(V) \cdot H(y - h(x)) = 0 \tag{5}$$

where $H(y - h(x)) = 1$ if $y \leqslant h(x)$ or zero otherwise and where $h(x)$ defines the adhesion profile (see figure 3). As no local rotation appears when nails grow, the conservation of angular momentum imposes that:

$$f_{x,y}(x,y) = f_{y,x}(x,y) \tag{6}$$

Hence the 2D stress tensor is symmetrical. To fully define the problem, boundary conditions need to be added, and two of those can be defined. We first assume that the growth stress $f_0(x)$ is only defined at the origin on the y-axis (i.e. proximal side) and has direction along the y-axis. This first boundary condition leads to:

$$f_{y,y}(x,0) = -f_0(x) \tag{7}$$

Furthermore, let us assume that no force is applied distally i.e. that the nail has a free distal edge. Therefore two further conditions follow (see appendix 1):

$$f_{x,x}(x, h'(x)) \cdot \partial_x h'(x) = f_{x,y}(x, h'(x)) \tag{8}$$

$$f_{y,y}(x, h'(x)) = \partial_x h'(x) \cdot f_{x,y}(x, h'(x)) \tag{9}$$

From the geometry of the nail (i.e. its symmetrical shape), it is obvious that the stresses will have to follow some important symmetry conditions. Figure 3(C) enounces all the symmetries with regard to the stresses:

$$\begin{aligned} f_{x,x}(-x,y) &= f_{x,x}(x,y) \\ f_{y,y}(-x,y) &= f_{y,y}(x,y) \\ f_{y,x}(-x,y) &= -f_{y,x}(x,y) \\ \partial_y f_{x,y} &= 0 \end{aligned} \tag{10}$$

The set of equations (4)–(10) defines the physical stresses present in a growing nail.

Stress solutions

Let us consider a solid nail growing at a constant velocity, V. Without further assumptions and using the set of equations (4)–(10) it is possible to determine the components of the stress tensor analytically. To this end, let us consider

equations (5) & (7) and integrate equation (5) over the 'y' variable. By virtue of $\partial_y f_{x,y} = \partial_y f_{y,x} = 0$ (i.e. $f_{y,x}$ is independent of the 'y' variable—see equation (10)). One obtains:

$$f_{y,y}(x, y) = -f_0(x) + f_{adh}(V)\int_0^y H(u - h(x))du - \partial_x f_{y,x}(x) \times y \quad (11)$$

Replacing equation (11) into the boundary condition given by equation (9) leads to:

$$f_{y,x}(x) = f_{y,x}(0) + \frac{1}{h'(x)}\int_0^x \left[-f_0(u) + f_{adh}(V)h(u)\right]du \quad (12)$$

Provided the adhesion profile of the nail and the profile of the distal edge, equation (12) completely determines $f_{x,y}(x)$ and, by symmetry, $f_{y,x}(x)$. As $f_{y,x}(x)$ is an odd function (equation (10)), the shear stress in x = 0 has to be null and as a result: $f_{y,x}(0) = 0$. Therefore, $f_{x,y}(x)$ and, by symmetry, $f_{y,x}(x)$ are now fully determined. Replacing equation (12) into equation (11) allows us to complete the determination of, $f_{y,y}(x, y)$, as follow:

$$\begin{aligned} f_{y,y}(x, y) = {} & -f_0(x)\left(1 - \frac{y}{h'(x)}\right) \\ & + h(x)f_{adh}(V)\left[\frac{\int_0^y H(u - h(x))du}{h(x)} - \frac{y}{h'(x)}\right] \\ & + \frac{y}{h'(x)}\partial_x h'(x) \\ & \times \int_0^x \left[-f_0(u) + h(u)f_{adh}(V)\right]du \end{aligned} \quad (13)$$

Using equation (4) together with $\partial_y f_{x,y}(x) = 0$ (equation (10)) allows one to determine that: $\partial_x f_{x,x} = 0$, namely that $f_{x,x}$ is only dependent on the variable 'y', i.e. is constant along the *x*-axis for a given value on the *y*-axis. As $f_{x,x}$ is only a function of the variable 'y', it is convenient to introduce 'y' using the reciprocal function, 'h'^{-1}' of the edge equation defined as $h'^{-1}(h'(x)) = x$. Therefore, using the boundary condition given by equation (8) allows the full determination of, $f_{x,x}$:

$$\begin{aligned} f_{x,x}(x, y = h'(x)) &= \frac{f_{x,y}(x)}{\partial_x h'(x)} \\ &= \partial_y h'^{-1}(y) \times f_{x,y}\left(h'^{-1}(y)\right) \end{aligned} \quad (14)$$

As a result, provided the shapes of the adhesion profile and edge of a nail, with the set of equations that have been determined so far, it is possible to determine the stress tensor components without any ambiguity. It is worth noting here that it is only when the growth and adhesion stresses do not compensate each other, i.e. $-f_0(u) + f_{adh}(V)h(u) \neq 0$, that $f_{y,x}$ and $f_{x,x}$ differ from zero. In turn this could lead to some pathological conditions

The normal case

Let us first consider a nail that is trimmed in such a way that: $h'(x) = h(x)$ and which has a growth profile given by: $f_0(x) = f_{adh}(V)h(x)$. In this case, one finds:

$$\begin{aligned} f_{x,x} &= f_{x,y} \\ &= 0 \\ f_{y,y}(x, y) &= -f_0(x)\left(1 - \frac{y}{h(x)}\right) \end{aligned} \quad (15)$$

Equation (15) shows that the only existing stress is linked to the growth stress. Such a stress should define the natural longitudinal curvature, i.e. the claw shape, of any growing nail.

The pathological case

Let us now consider a nail that is trimmed in such a way that: $h'(x) = h(x)$ and that has an imbalanced growth profile such that: $F(x) = -f_0(x) + f_{adh}(V)h(x) \neq 0$. In this case, one shall assume also that, $F(x)$, is small and is an even function of the variable 'x' to preserve the conditions regarding the symmetry of the nail. As a result, $F(x)$ can be developed using Taylor series as follow: $F(x) = F(0) + \sum_{i=1}^{\infty}\partial_{x^{2i}}F\,|_{x=0}\, x^{2i}/2i!$. Naturally, each term in the later development is expected to be small compared to the leading term. Applying the same operation to the equation of the edge, $h'(x) = h(x) = h(0) + \sum_{i=1}^{\infty}\partial_{x^{2i}}h\,|_{x=0}\, x^{2i}/2i!$, and replacing the Taylor series of $F(x)$ and $h'(x) = h(x)$ into equations (11), (12) and (13), leads to:

$$\begin{aligned} f_{y,x}(x) &= \frac{F(0)x}{h(0)}\alpha(x) \\ f_{x,x}(x) &= \frac{F(0)}{h(0)\partial_{x^2}h\,|_{x=0}}\beta(x) \\ f_{y,y}(x, y) &= -f_0(x)\left(1 - \frac{y}{h(x)}\right) \\ &\quad + yx^2\frac{\partial_{x^2}h\,|_{x=0}\,F(0)}{h(0)}\gamma(x) \end{aligned} \quad (16)$$

where the expression of $\alpha(x)$, $\beta(x)$ and $\gamma(x)$ are given in appendix 2 and where $\alpha(0) = \beta(0) = \gamma(0) = 1$. We note here that for nails having very flat distal edges, i.e. when: $\partial_{x^2}h\,|_{x=0} \ll 1$, the stress component that will dominate over all the others in the distal part of the nail (the yellow and blue parts in figure 3(B)) is: $f_{x,x}(x)$[2]. This result suggests that nails with a flat profile such as those the big toe should be more prone to distal transverse stresses, if the difference between the growth and adhesion stresses is not properly balanced.

[2] As by definition: $f_{x,x} = f_{x,y}/\partial_x h$ (equation (14)), it follows that for flat profiles the edge equation musty verifies $\partial_x h \ll 1$ and therefore, $f_{x,x} \gg f_{x,y}$. From equation (13) and $\partial_x h \ll 1$, it follows that $f_{y,y} \sim -f_0(x)(1 - y/h(x))$. As in the distal part of a flat nail $y \sim h(x)$, one can assume $f_{y,y} \sim 0$ or at least very small. Note that these results do not hold when the nail has not a flat profile.

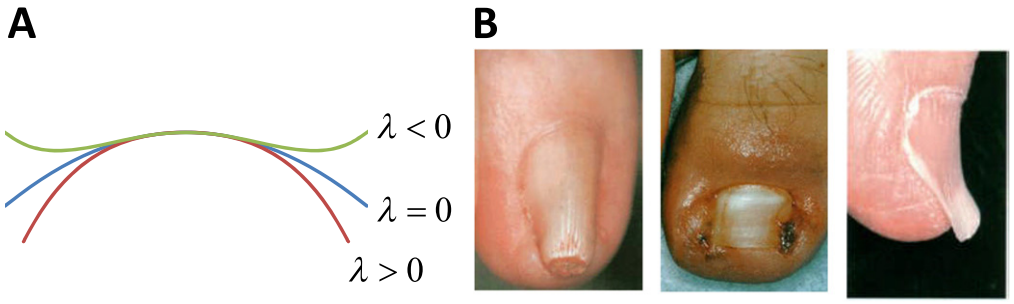

Figure 4. Nail shape and related conditions. **(A)** Transverse profile of the distal part of a nail for different sign of λ. **(B)** Photos of nail conditions: pincer nail (left), ingrown nail (middle) and spoon-shaped nail (right); photos from Baran R *et al* (2014).

Application to ingrown nails: why the big toe?

The ingrowing nail or 'onychocryptosis' is a condition causing much discomfort and morbidity in school children/adolescents/young adults (Khunger and Kandhari 2009) and is diagnosed in 15% of pregnant women (Ponnapula and Boberg 2010). Though recognized for a long time, a satisfactory treatment of onychocryptosis remains elusive, in part, because the aetiology for ingrown nails is not understood. Different theories were initially proposed and classified according to whether the primary fault is based on the nail plate or not (Haneke 2008). However a structural abnormality of the nail plate has been ruled out (Pearson *et al* 1987), but it was demonstrated instead, that a change in the transverse curvature of the nail plate (i.e. curvature along the x-axis) located distally promotes the condition (Pearson, Bury, Wapples and Watkin 1987). As a transverse curvature of the nail plate is involved, this suggests in turn, that some mechanical consideration may be underlie the aetiology of onychocryptosis.

It is well known that ingrown nail occurs predominantly in the big toe. From a physical point of view one central difference between the big toe and all other toes or fingers is the fact that the adhesion profile of the nail plate is remarkably flat (but not straight—as otherwise the boundary conditions defined by equation (8) and (9) would not apply). As seen above, this means that the transverse stress $f_{x,x}$ is the leading stress in the distal part of the nail. If an exaggerated distal curvature of the nail defines the ingrown nail, it is central to determine how the curvature is related to the transverse stress.

To determine how the shape of the nail is affected we concentrate on the energies method.

As $f_{x,x}$ is the leading stress in the distal part of the nail, the potential energy of the nail can be simplified to $E_1 \sim \iint f_{x,x}\,\mathrm{dS}$ where the integration is performed over the nail surface area. As the potential energy is transformed into a bending energy to impose a new configuration to the nail and that, ingrown nails are diagnosed by a change in the transverse curvature (i.e. along the x-axis—see figure 4(B)) and not by longitudinal curvature (i.e. not along the y-axis), it is legitimate to assume that the only curvature involved is the one along the x-axis. In these conditions, Kirchhoff's theory of plate bending allows us to rewrite the bending energy under the form (Helfrich 1973, Ventsel and Krauthammer 2001): $E_2 = \frac{D}{2}\iint \left(C_x - C_0\right)^2 \mathrm{dS}$, where the integration is performed over the nail surface and where, $D = Ye^3/12(1-\upsilon)$, is the flexural rigidity of the nail plate (Y, is the Young modulus assumed to be isotropic across the nail and; υ the Poisson's coefficient), C_x, the transverse curvature of the nail surface along the x-axis and, C_0, the spontaneous curvature of the nail that is identical to the curvature of the finger[3]. For small deformations, it is convenient to describe the nail using the Monge gauge, i.e. by its height $z' = w(x', y')$, with respect to a reference plane where x' and y' are the Cartesian coordinates in the reference plane. As $dx'dy' = dS'$ and dS are related together by: $dS = \sqrt{\left[1 + (\partial w/\partial x')^2\right]\left[1 + (\partial w/\partial y')^2\right]}\,\mathrm{dS}'$, making use of the small deformation hypotheses: $\partial_y w \sim \partial_y{}^2 w \sim 0$ and of $\left|\partial_{x'} w\right| \ll 1$ and $e\left|\partial_{x'^2} w\right| \ll 1$; it is possible to rewrite the sum of energies to the leading orders in the displacement along the z'-axis as follows:

$$E_1 + E_2 \sim \iint \frac{D}{2}\left(\frac{\partial^2 w}{\partial x'^2} - C_0\right)^2 + f_{x,x}(y')\left[1 + \frac{1}{2}\left(\frac{\partial w}{\partial x'}\right)^2\right]\mathrm{dS}' + \iint o\left(\frac{\partial^3 w}{\partial x'^3}; \left(\frac{\partial w}{\partial x'}\right)^3\right)\mathrm{dS}' \tag{17}$$

Finally, removing the superscript prime (i.e. " ' ") as all the physical variables are now expressed in the fix Cartesian referential, the Euler–Lagrange method determines the equation of the nail shape (see appendix 3):

$$\partial_{x^4} w - \lambda(y)\partial_{x^2} w = 0 \tag{18}$$

where $\lambda(y) = f_{x,x}(y)/D$. Using Fourier series with the following initial conditions: $w\,|_{x=0} = w_0$, $\partial_x w\big|_{x=0} = 0$ and $\partial_x{}^2 w\big|_{x=0} = C_0$ leads to the 'ingrown nail equation':

$$w(x, y) = w_0 + \frac{C_0}{\lambda(y)}\left[\cosh\left(x\sqrt{\lambda(y)}\right) - 1\right] \tag{19}$$

[3] Nails are composed of dead cells that grow from soft tissues and therefore it is legitimate to assume that any nail should take the shape of the finger in normal conditions.

Let us assume that $\sqrt{\lambda(y)} \ll 1/l$, where l is the width of the nail, one finds: $w(x, y) \sim w_0 + \frac{C_0}{2}x^2\left[1 + \frac{\lambda(y)}{12}x^2\right]$. This last relation shows that the sign of $\lambda(y)$ (i.e. the sign of $f_{x,x}(y)$) will influence the sign of the curvature as seen in figure 4(A). As $f_{x,x}(y) = \frac{F(0)}{h(0)\partial_x 2h\,|_{x=0}}\beta(h^{-1}(y))$, the leading term of $f_{x,x}(y)$, i.e. $F(0) = -f_0(0) + f_{adh}(V)h(0)$, can change sign depending onto whether the growth stress is larger or smaller than the adhesion stress.

Influence of trimming on nail conditions

$f_{x,x}(y)$ is defined by the boundary condition given by equation (14) and, as a result, exists only when the distal edge of the nail is slightly curved. Therefore, cutting the nail in a straight way, i.e. removing the slight curvature, and maintaining this profile over time should remove $f_{x,x}(y)$ and therefore improve the ingrown nail condition.

Conversely, bad trimming of the distal part of the nail may amplify the magnitude of, $f_{x,x}(y)$. To demonstrate this point, assume in this case that the distal part is trimmed such that $h'(x) = h'(0) - a(2x/l)^{2m}$. If $F(x) \neq 0$, from equation (14) the transverse stress can be rewritten as, $f_{x,x} \sim [a/(h'(0) - y)]^{\frac{m-1}{m}}$, showing that the magnitude of the transverse stress can be very high. This suggests that careful attention should be given to the different ways of trimming nails to avoid the worsening of nail conditions involving the transverse curvature.

Discussion

It has been known since the time of Hippocrates that a particular change in nail shapes can signify specific underlying conditions (Myers and Farquhar 2001). From a physical point of view, nail growth and shape are necessarily inter-related. Therefore, it seemed important to investigate whether physics could play a role in, and as a result explain, the aetiology of some nail conditions.

As our daily experience of nail suggests that the nail plate is hard and therefore should be considered as a solid we have modelled both the adhesion and balance of stresses in this 2D system. When diseased nails are surgically removed, their shapes remain the same and as a result we made the implicit assumption that the nail adapts the unbalanced stresses by changing shape over time. To conclude, the model suggests that the imbalance between the growth and adhesion stresses is responsible for changing the distal transverse curvature of nails, and confirms that it is the big toe that is predominantly afflicted by nail conditions of mechanical origin due to its flat profile.

This important result seems to agree relatively well with observations in the field of nail conditions. For example, in man, the term pincer nails (figure 4(B) left) describes an exaggerated transverse curvature of the nail plate along the longitudinal axis (Baran *et al* 2001, Cornelius and Shelley 1968). This condition is mostly acquired during advanced age (Lee *et al* 2008). Although the aetiology is not fully understood a change in nail growth related to a weaker growth force with advanced age has been suggested (de Berker *et al* 2007). The other well known condition, the ingrown nail (figure 4(B) middle), is often diagnosed in school children/adolescents/young adults (Khunger and Kandhari 2009) and pregnant women (Ponnapula and Boberg 2010). It is remarkable that this condition occurs in patients where metabolic growth is active. For example, in pregnancy, periods of high sex hormone productions are well known to accelerate nail growth (Hewitt and Hillman 1966, Ponnapula and Boberg 2010). A last condition referred to as 'spoon-shaped nails' corresponds to an inverted curvature of the nail (figure 4(B) right). This shape can be described by the model. Indeed, such a condition, which occurs in newborns or in brittle nails, is expected to appear when the growth stress is small enough to allow the curvature inversion (so that $\lambda(y) < 0$) and/or the nail is thin enough and thus brittle (Fawcett *et al* 2004) as $\lambda(y) \propto 1/e^3$. This shape is also predicted if the adhesion of the nail drops, possibly as a result of aging.

Each condition cited above is diagnosed based on the shape of the nail. These shapes can be modelled by a set of physical equations suggesting that pincer, ingrown and spoon-shaped nails are interrelated conditions forming a continuum. In this context, physics suggests that the imperfection in nail growth, possibly due to aging and/or metabolic changes, can precisely define the aetiology of some nail conditions. Finally, although it seems that any condition should recover with time, the trimming has great importance, and should be carefully monitored, especially with the increasing number of nail salons.

Conclusion

We suggest that some nail conditions affecting the nail shape can be explained by first principles. These are thus not disparate conditions but form a continuum of natural conditions.

Acknowledgements

The research was funded by the University of Nottingham and Vertex Pharmaceuticals. The authors declare no conflict of interests and would like to thank Professor Oliver E Jensen for fruitful discussions; Florence Hillen and Emily Paul for proof reading the manuscript; and Ramzi Al-Agele for providing horse materials.

Appendix A. balance of stresses and boundary conditions

We consider the square a given by figure 3(B.1) to determine the balance of stresses and focus on the y-axis. The balance of stresses gives $\partial_y f_{y,y}(x, y) + \partial_x f_{y,x}(x, y) - f_{adh}(V)\cdot$

$H(y-h(x))=0$, where $H(y-h(x))=1$ if $y \leqslant h(x)$ or zero otherwise. Integrating this equation over the y-axis gives:

$$f_{y,y}(x,y) = f_{y,y}(x,0) - \int_0^y \left[\partial_x f_{y,x}(x,y) - f_{adh}(V)\cdot H(y-h(x))\right]\mathrm{d}y \quad \text{(A1.a)}$$

Where $f_0(x) = -f_{y,y}(x,0)$ as defined in the text. Assuming further that no force is applied on the distal edge of the nail, one finds:

$$\left\{\left[f_{i,j}(x,h(x))\right]\vec{n}\right\}\cdot\vec{e}_y = f_{y,x}(x,h'(x))n_x + f_{y,y}(x,h'(x))n_y = 0 \quad \text{(A1.b)}$$

where $\vec{n}\sqrt{1+\partial_x h'(x)^2} = -\partial_x h'(x)\vec{e}_x + \vec{e}_y$. The balance of stresses along the x-axis can be determined similarly:

$$\partial_x f_{x,x}(x,y) + \partial_y f_{x,y}(x,y) = 0 \quad \text{(A1.c)}$$

As one assumes that no stress is applied over the x-axis the only relation regarding the boundary condition of the distal edge, is:

$$\left\{\left[f_{i,j}(x,h(x))\right]\vec{n}\right\}\cdot\vec{e}_x = f_{x,x}(x,h'(x))n_x + f_{x,y}(x,h'(x))n_y = 0 \quad \text{(A1.d)}$$

as seen in the text.

Appendix B

$$\alpha(x) = \frac{1+\sum_{i=1}^{\infty}\partial_{x^{2i}}F\,|_{x=0}\,x^{2i}/F(0)(2i+1)!}{1+\sum_{i=1}^{\infty}\partial_{x^{2i}}h\,|_{x=0}\,x^{2i}/h(0)2i!}$$

$$\beta(x) = \frac{\left[1+\sum_{i=1}^{\infty}\partial_{x^{2i}}F\,|_{x=0}\,x^{2i}/F(0)(2i+1)!\right]}{\left[\sum_{i=1}^{\infty}\partial_{x^{2i}}h\,|_{x=0}\,x^{2(i-1)}/\partial_{x^2}h\,|_{x=0}\,(2i-1)!\right]}\times\frac{\left[\sum_{i=1}^{\infty}\partial_{x^{2i}}h\,|_{x=0}\,x^{2(i-1)}/\partial_{x^2}h\,|_{x=0}\,(2i-1)!\right]}{\left[1+\sum_{i=1}^{\infty}\partial_{x^{2i}}h\,|_{x=0}\,x^{2i}/h(0)2i!\right]}$$

$$\gamma(x) = \frac{\left[1+\sum_{i=1}^{\infty}\partial_{x^{2i}}F\,|_{x=0}\,x^{2i}/F(0)(2i+1)!\right]}{\left[1+\sum_{i=1}^{\infty}\partial_{x^{2i}}h\,|_{x=0}\,x^{2i}/h(0)2i!\right]}$$

Appendix C. Energy optimisation using the Euler–Lagrange method

Consider the free energy:

$$E_{tot}(w) \sim \iint \frac{D}{2}\left(\frac{\partial^2 w}{\partial x^2} - C_0\right)^2 + f_{x,x}(y)\left[1+\frac{1}{2}\left(\frac{\partial w}{\partial x}\right)^2\right]\mathrm{dS} \quad \text{(A3.a)}$$

One needs to find the function, w, that minimizes the free energy above. Let us perform a small variation of $w \to w+\delta w$. The concomitant change in the free energy is then:

$$\delta E_{tot} \sim \iint \frac{D}{2}\left(\frac{\partial^2 w}{\partial x^2} + \frac{\partial^2 \delta w}{\partial x^2} - C_0\right)^2 + f_{x,x}(y)\left[1+\frac{1}{2}\left(\frac{\partial w}{\partial x} + \frac{\partial \delta w}{\partial x}\right)^2\right]\mathrm{dS} - \iint \frac{D}{2}\left(\frac{\partial^2 w}{\partial x^2} - C_0\right)^2 + f_{x,x}(y)\left[1+\frac{1}{2}\left(\frac{\partial w}{\partial x}\right)^2\right]\mathrm{dS} \quad \text{(A3.b)}$$

Where $\delta E_{tot} = E_{tot}(w+\delta w) - E_{tot}(w)$. Working the energy difference to the first order of the small quantity δw one finds:

$$\delta E_{tot} \sim \iint D\left(\frac{\partial^2 w}{\partial x^2} - C_0\right)\frac{\partial^2 \delta w}{\partial x^2} + f_{x,x}(y)\left(\frac{\partial w}{\partial x}\frac{\partial \delta w}{\partial x}\right)\mathrm{dS} \quad \text{(A3.c)}$$

Splitting equation (A3.c) into two different integrals, i.e. over the curvature and the gradient of w one finds:

$$\iint D\left(\frac{\partial^2 w}{\partial x^2} - C_0\right)\frac{\partial^2 \delta w}{\partial x^2}\mathrm{dS} = \int\left\{\frac{\partial}{\partial x}\left[\left(\frac{\partial^2 w}{\partial x^2} - C_0\right)\frac{\partial \delta w}{\partial x}\right]\right\}_{-x_0}^{x_0}\mathrm{dy} - \int\left\{\frac{\partial}{\partial x}\left[\frac{\partial}{\partial x}\left(\left(\frac{\partial^2 w}{\partial x^2} - C_0\right)\delta w\right)\right]\right\}_{-x_0}^{x_0}\mathrm{dy} + \iint \frac{\partial^4 w}{\partial x^4}\delta w\mathrm{dS} \quad \text{(A3.d)}$$

And

$$\iint f_{x,x}(y)\frac{\partial w}{\partial x}\frac{\partial \delta w}{\partial x}\mathrm{dS} = \int f_{x,x}(y)\left\{\frac{\partial}{\partial x}\left[\frac{\partial w}{\partial x}\delta w\right]\right\}_{-x_0}^{x_0}\mathrm{dy} - \iint f_{x,x}(y)\frac{\partial^2 w}{\partial x^2}\delta w\mathrm{dS} \quad \text{(A3.e)}$$

Where the interval $[-x_0, x_o]$ is the interval of integration over the x-axis, i.e. the extend of the projection of the nail surface area over the x-axis contained in the Cartesian reference plane. Using the conditions of symmetry, namely that δw and w are even function of the variable 'x', from equations (A3.e) & (A3.d) it follows that δE_{tot} can be reduced to zero if:

$$\frac{\partial^4 w}{\partial x^4} - f_{x,x}(y)\frac{\partial^2 w}{\partial x^2} = 0 \qquad \text{(A3.f)}$$

References

Arnold M, Cavalcanti-Adam E A, Glass R, Blummel J, Eck W, Kantlehner M, Kessler H and Spatz J P 200 4 Activation of integrin function by nanopatterned adhesive interfaces *Chemphyschem.* **5** 383–8

Baran R, Dawber R, Haneke E, Tosti A and Bristow I 2014 *Informa Health Care* (Abingdon, Oxford: Taylor & Francis)

Baran R, Haneke E and Richert B 2001 Pincer nails: definition and surgical treatment *Dermatol. Surg.* **27** 261–6

Benz A, Zenker W, Hildebrandt T B, Weissengruber G, Eulenberger K and Geyer H 2009 Microscopic morphology of the elephant's hoof *J. Zoo Wildl Med.* **40** 711–25

Butler K D Jr and Hintz H F 1977 Effect of level of feed intake and gelatin supplementation on growth and quality of hoofs of ponies *J. Anim. Sci.* **44** 257–61

Cavalcanti-Adam E A, Micoulet A, Blummel J, Auernheimer J, Kessler H and Spatz J P 2006 Lateral spacing of integrin ligands influences cell spreading and focal adhesion assembly *Eur. J. Cell Biol.* **85** 219–24

Cavalcanti-Adam E A, Volberg T, Micoulet A, Kessler H, Geiger B and Spatz J P 2007 Cell spreading and focal adhesion dynamics are regulated by spacing of integrin ligands *Biophys. J.* **92** 2964–74

Cornelius C E III and Shelley W B 1968 Pincer nail syndrome *Arch. Surg.* **96** 321–2

de Berker D A, Andre J and Baran R 2007 Nail biology and nail science *Int. J. Cosmet. Sci.* **29** 241–75

Dembo M, Torney D C, Saxman K and Hammer D 1988 The reaction-limited kinetics of membrane-to-surface adhesion and detachment *Proc. of the Royal Society of London Series B-Biological Sciences* vol 234, pp 55–83

Dong C and Lei X X 2000 Biomechanics of cell rolling: shear flow, cell-surface adhesion, and cell deformability *J. Biomech.* **33** 35–43

Eliashar E 2012 The biomechanics of the equine foot as it pertains to farriery *Veterinary Clinics of North America-Equine Practice* **28** 283

Fawcett R S, Linford S and Stulberg D L 2004 Nail abnormalities: clues to systemic disease *Am. Fam. Physician* **69** 1417–24

Godwin K O 1959 An experimental study of nail growth *Journal of Nutrition* **69** 121–7

Haneke E 2008 Controversies in the treatment of ingrown nails *Dermatol. Res. Pract.* 783924

Harrison S M, Monahan F J, Zazzo A, Bahar B, Moloney A P, Scrimgeour C M and Schmidt O 2007 Three-dimensional growth of bovine hoof as recorded by carbon stable isotope ratios *Rapid Commun. Mass Spectrom.* **21** 3971–6

Helfrich W 1973 Elastic properties of lipid bilayers—theory and possible experiments *Zeitschrift Fur Naturforschung C-A Journal of Biosciences* **C28** 693–703

Hewitt D and Hillman R W 1966 Relation between rate of nail growth in pregnant women and estimated previous general growth rate *Am. J. Clin. Nutr.* **19** 436–9

Johnston A M and Penny R H C 1989 Rate of claw horn growth and wear in biotin-supplemented and non-supplemented pigs *Veterinary Record* **125** 130–2

Khunger N and Kandhari R 2009 Ingrown toenails *Indian J. Dermatol. Venereol. Leprol.* **78** 279–89

Lee J I, Lee Y B, Oh S T, Park H J and Cho B K 2008 A clinical study of 35 cases of pincer nails *Ann. Dermatol.* **23** 417–23

Miller K V, Marchinton R L and Nettles V F 1986 The growth rate of hooves of white-tailed deer *J. Wildl Dis.* **22** 129–31

Myers K A and Farquhar D R 2001 The rational clinical examination. Does this patient have clubbing? *JAMA* **286** 341–7

Pearson H J, Bury R N, Wapples J and Watkin D F 1987 Ingrowing toenails: is there a nail abnormality? A prospective study *J. Bone Joint Surg Br.* **69** 840–2

Pollitt C C 1994 The basement-membrane at the equine hoof dermal-epidermal junction *Equine Veterinary Journal* **26** 399–407

Ponnapula P and Boberg J S 2010 Lower extremity changes experienced during pregnancy *J. Foot Ankle Surg.* **49** 452–8

Ra H J, Picart C, Feng H S, Sweeney H L and Discher D E 1999 Muscle cell peeling from micropatterned collagen: direct probing of focal and molecular properties of matrix adhesion *Journal of Cell Science* **112** 1425–36

Reboux S, Richardson G and Jensen O E 2008 Bond tilting and sliding friction in a model of cell adhesion *Proc. of the Royal Society a-Mathematical Physical and Eng. Sciences* vol 464, pp 447–67

Shelton J, Usherwood N M, Wapenaar W, Brennan M L and Green L E 2012 Measurement and error of hoof horn growth rate in sheep *Journal of Agricultural Science* **150** 373–8

Telezhenko E, Bergsten C, Magnusson M and Nilsson C 2009 Effect of different flooring systems on claw conformation of dairy cows *J. Dairy Sci.* **92** 2625–33

Thoefner M B, Wattle O, Pollitt C C, French K R and Nielsen S S 2005 Histopathology of oligofructose-induced acute laminitis in heifers *J. of Dairy Science* **88** 2774–82

Ventsel E and Krauthammer T 2001 *Thin Plates and Shells: Theory, Analysis and Applications* (Boca Raton, FL: CRC Press)

Worth D C and Parsons M 2008 Adhesion dynamics: mechanisms and measurements *Int. J. Biochem. Cell Biol.* **40** 2397–409